Vascular Pharmacology 121 (2019) 106577

Contents lists available at ScienceDirect

Vascular Pharmacology

journal homepage: www.elsevier.com/locate/vph

Antiretroviral drug-induced endothelial dysfunction is improved by dual PPARα/γ stimulation in obesity

Festus Kamau (MBChB; PhD)[a,*], Hans Strijdom (MBChB; PhD)[a], Peter Mwangi (B.Pharm; PhD)[b], Dee Blackhurst (PhD)[c], Emiliana Imperial (MSc)[a], Ruduwaan Salie (PhD)[a,d]

[a] Division of Medical Physiology, Faculty of Medicine and Health Sciences, Stellenbosch University, PO Box 241, Cape Town 8000, South Africa
[b] Department of Medical Physiology, School of Medicine, College of Health Sciences, University of Nairobi, P.O. Box 30197, 00100 Nairobi, Kenya
[c] Division of Chemical Pathology, Faculty of Health Sciences, University of Cape Town, Cape Town 7925, South Africa
[d] The Biomedical Research and Innovation Platform (BRIP), South African Medical Research Council, PO Box 19070, Tygerberg 7505, South Africa

ARTICLE INFO

Keywords:
Obesity
Highly active antiretroviral therapy (HAART)
PPARα/γ agonist
Saroglitazar
Endothelial dysfunction

ABSTRACT

Obesity rates are rising in HIV-infected populations; however, the putative role of highly active antiretroviral therapy (HAART) in the development of endothelial and cardiovascular derangements in the presence of pre-existing overweight/obesity is unclear. Although dual peroxisome proliferator-activated receptors-alpha/gamma (PPARα/γ) stimulation mitigates HAART-induced metabolic dysfunction, vascular effects are unresolved. To investigate whether HAART induces vascular dysfunction in obesity and to explore the underlying mechanisms of PPARα/γ stimulation, male Wistar rats were placed on a high-calorie diet for 16 weeks. After 10 weeks, HAART (lopinavir/ritonavir, azidothymidine/lamivudine) with/without PPARα/γ agonist, Saroglitazar, was administered daily for six weeks. Excised thoracic aorta rings were subjected to isometric tension studies and Western blot measurements. HAART + Saroglitazar-treated obese animals recorded lower adiposity indices (4.3 ± 0.5%) vs. HAART only-treated obese rats (5.6 ± 0.3%; $p < .01$). Maximum acetylcholine-induced vasorelaxation (R_{max}), was lower in obese + HAART group (76.10 ± 3.58%) vs. obese control (101.40 ± 4.75%; $p < .01$). However, R_{max} was improved in obese + HAART + Saroglitazar (101.00 ± 3.12%) vs. obese + HAART rats ($p < .001$). The mean $LogEC_{50}$ was improved in obese + HAART + Saroglitazar vs. obese + HAART group; $p = .003$. Improved endothelial function in obese + HAART + Saroglitazar group was associated with upregulation of eNOS, PKB/Akt and downregulated p22-phox expression vs. obese + HAART group. Therefore, PPARα/γ stimulation attenuated HAART-induced endothelial dysfunction by upregulating vasoprotective eNOS, PKB/Akt signaling and downregulating pro-oxidative p22-phox expression.

Abbreviations: 3TC, 2,3′ dideoxy- 3-thiacytidine (Lamivudine); AI, adiposity index; AMPK, adenosine monophosphate-activated protein kinase; ANOVA, analysis of variance; AZT, Zidovudine; BMI, body mass index; BRIP, Biomedical Research and Innovation Platform; CD, conjugated dienes; CVD, cardiovascular disease; ELISA, enzyme-linked immunosorbent assay kit; eNOS, endothelial nitric oxide synthase; ERK1/2, extracellular-signal-regulated protein kinase; FBG, fasting blood glucose; FMD, flow-mediated dilatation; HAART, Highly active antiretroviral therapy; HCD, High-calorie diet; HDL-C, high-density lipoprotein cholesterol; HIV, human immunodeficiency virus; HMG-CoA, 3-hydroxy-3-methyl-glutaryl-coenzyme A reductase; HOMA-IR, homeostasis model assessment for insulin resistance; IP, intraperitoneal; JNK, c-Jun N-terminal kinase; L-NAME, L-nitroarginine methyl ester; LDL-C, low-density lipoprotein cholesterol; LPV/r, lopinavir boosted with ritonavir; NRTI, nucleoside reverse transcriptase inhibitor; PARP, poly (adenosine diphosphate, ADP-ribose) polymerase; PGC-1 α, peroxisome proliferator-activated receptor gamma coactivator 1-alpha; PI, protease inhibitors; PKB/Akt, protein kinase B; PPARα/γ, peroxisome proliferator-activated receptors-alpha/gamma; RBG, random blood glucose; SAMRC, South African Medical Research Council; SAPK, stress-activated protein kinase; SD, supplemental document; T2DM, Type-2 diabetes mellitus; TBARS, thiobarbituric acid reactive substances; TBM, Total body mass; TC, total cholesterol; TG, triglyceride; TZD, thiazolidinedione

* Corresponding author.
E-mail addresses: 19240430@sun.ac.za (F. Kamau), jgstr@sun.ac.za (H. Strijdom), peterwaweru@uonbi.ac.ke (P. Mwangi), dee.blackhurst@uct.ac.za (D. Blackhurst), emeliana.imperial@yahoo.com (E. Imperial), ruduwaan.salie@mrc.ac.za (R. Salie).

https://doi.org/10.1016/j.vph.2019.106577
Received 9 April 2019; Received in revised form 15 June 2019; Accepted 3 July 2019
Available online 05 July 2019

List of units of measurements

%	Percentage
°C	Degree Celsius
dL	Decilitre
g	Gram
IU	International units
kDa	Kilo Dalton
kg	Kilogram
L	Litre
M	Molar
mg	Milligram
mL	Millilitre
mm	Millimetre
mmol	Millimol
ng	Nanogram
nM	Nanomolar
μ	Micro
μL	Microlitre
μM	Micromolar
μmol	Micromol

1. Introduction

The introduction of highly active antiretroviral therapy (HAART) has successfully reversed the high mortality associated with HIV/AIDS-related opportunistic infections, malignancies, severe wasting and malnutrition [1,2]. Indeed, the lifespan of HIV-infected adults compliant with various HAART regimens now approximates that of non-infected persons [3]. However, this chronicity has led to a surge in both incidence and prevalence of non-communicable diseases such as cardiovascular disease (CVD), metabolic derangements, overweight/obesity and type-2 diabetes mellitus (T2DM) [4,5]. New evidence suggests that long-term HAART is associated with added CVD risk and results in poorer outcomes compared to HIV-free persons [6,7].

An increase in the prevalence of overweight/obesity (based on body mass index, (BMI)) has been reported in HIV-infected populations before they commence HAART [8,9]. Consequently, the prevalence of metabolically unhealthy, overweight/obese HIV-infected individuals is rising [10]. Additionally, HAART per se is also associated with obesity and related metabolic derangements, characterised by dyslipidemia and ectopic fat deposition in visceral organs such as the liver, blood vessels and the heart [5,11]. Previous studies focussed on metabolic dysregulation that acts as a prequel to vascular and cardiac impairment; however, limited studies evaluated vascular dysfunction in HAART. Importantly, antiretroviral therapy in HIV infection has been directly implicated in endothelial dysfunction [12–14] and vascular inflammation (vasculitides) with subsequent loss of vascular integrity and the development of multiple aneurysms and occlusion [15].

There are controversies as to whether HAART is protective or detrimental to vascular integrity: using flow-mediated dilatation (FMD) techniques, protective effects of HAART have been reported [16] whereas Stein and colleagues [17], implicated protease inhibitors (PI) in inducing pro-atherogenic dyslipidemia and endothelial dysfunction. Direct PI-and nucleoside reverse transcriptase inhibitor (NRTI)-induced endothelial dysfunction has also been reported in rats [13]. It is therefore evident that chronic antiretroviral-mediated endothelial dysfunction may occur with or without pro-atherogenic dyslipidemia. The mechanisms implicated in this impairment include mitochondrial dysfunction and increased oxidative stress which precede overt atherosclerosis [14,18].

Various strategies (lifestyle and pharmacological) have been employed to mitigate metabolic derangements induced by diet and HAART. Lipid/cholesterol lowering agents such as 3-hydroxy-3-methylglutaryl-coenzyme A reductase (HMG-CoA) inhibitors (statins), PPARα agonists (fibrates), PPARγ agonists (thiazolidinediones) and ezetimibe ameliorate dyslipidaemia and lipodystrophy [19–21]. However, aggravated risks of drug-drug interactions and hepatotoxicity limit their use [20,22]. Recently, a novel, nonthiazolidinedione (TZD) and non-fibric acid derivative, dual PPARα/γ agonist (Saroglitazar, [(*S*)-α-ethoxy-4-{2-[2-methyl-5-(4-methylthio)phenyl)]-1H-pyrrol-1-yl]-ethoxy})-benzenepropanoic acid magnesium salt]) was introduced for dyslipidemia management in T2DM [23]. In HIV-infected patients with dyslipidemia, Saroglitazar improves lipid profile and has a favorable toxicity profile [24]. However, experimental studies on vascular/endothelial function have not been conducted and the impact of endothelial dual PPARα/γ stimulation in HAART is unknown.

In view of the aforementioned literature, we hypothesized that dual PPARα/γ stimulation will limit vascular endothelial dysfunction in a pre-existing diet-induced obese rat model exposed to HAART. The overarching aim of the present study was to investigate whether the introduction of a PI-based HAART regimen in obesity induces endothelial dysfunction and to evaluate the role of dual PPARα/γ stimulation as a potential therapeutic target to limit possible adverse HAART effects and to explore the underlying putative pathophysiologic mechanisms.

2. Materials and methods

Ethics approval was granted by the Stellenbosch University Animal Research Ethics Committee (Protocol #: SU-ACUD15–00019) and animals were handled in strict adherence to ARRIVE guidelines and South African national standards (SANS10386:2008).

2.1. Study design

We employed a randomised controlled experimental study design, where 128 (seven to eight week-old) male pathogen free Wistar rats were randomly allocated into two groups (n = 64/group) and fed (for 16 weeks) on either standard rat chow composed of 4.8% fat, 17.1% protein, 34.6% carbohydrates and 5.3% sucrose or rat chow and specially formulated high-calorie diet (HCD) composed of 11.5% fat, 8.3% protein, 42% carbohydrate and 20% sucrose [25]. The diet composition was analyzed by Microchem specialized laboratory services (Cape Town, South Africa). All animals had ad libitum access to water and food, were housed at standard day-night cycles of 12 h, temperatures of 22 °C and 40% humidity and individual total body mass (TBM) was monitored weekly. At the eleventh week, each group was further randomly divided into four subgroups (n = 16/group, see below) and treated with HAART and/or Saroglitazar for six weeks (daily oral gavage between 9:00–11:00 a.m.) at human equivalent doses calculated using the body weight/surface area normalization formula [26].

a) Vehicle, distilled water – control group
b) HAART (PI: Lopinavir (68.57 mg/kg/day) boosted with ritonavir (17.14 mg/kg/day) (LPV/r) -Aluvia™ (AbbVie (Pty) Ltd. South Africa). + NRTIs: Zidovudine, AZT (51.43 mg/kg/day)/ Lamivudine, 3TC (25.71 mg/kg/day) - COMBIVIR® (GlaxoSmithKline South Africa (Pty) Ltd).
c) HAART + PPARα/γ agonist (Saroglitazar), Lipaglyn™ (0.40 mg/kg/day) (Zydus Discovery: A division of Cadila Healthcare Limited, India).
d) Saroglitazar

Following completion of the feeding and treatment programs, each of the eight groups was further randomly divided into two (n = 8/group). Eight rats were fasted overnight (only accessed water ad libitum) and subjected to euthanasia by intraperitoneal (IP) injection of 160 mg/kg of sodium pentobarbitone (Eutha-naze®, Bayer (Pty) Ltd. South Africa), after which a thoracotomy was performed, the thoracic aorta incised, and pooled blood collected for subsequent biochemical analyses. The remaining animals (n = 8/group) were euthanised for the harvesting of aortic tissue to perform aortic ring isometric tension studies and Western blot protein measurements. IP fat was also

Table 1
Biometric measurements and biochemistry.

Variable	n/group	Lean Control	HCD Control	Lean HAART	HCD HAART	Lean HAART + Saro	HCD HAART + Saro	Lean Saro	HCD Saro
TBM (g) week 10	16	320.4 ± 9.4	362.6 ± 10.2 [a]**	322.4 ± 7.7	358.0 ± 10.1 [b]**	318.1 ± 8.5	358.3 ± 9.9 [c]**	319. 6 ± 7.4	354 ± 12.1[d]**
TBM (g) week 16	16	350.3 ± 10.1	416.1 ± 14.4[a]**	358.2 ± 6.4	399.1 ± 15.9[b]**	355.2 ± 6.5	389.4 ± 7.1[c]**	354.6 ± 7.7	398.1 ± 10.6[d]**
AI (% IP fat)	16	3.4 ± 0.3	6.3 ± 0.3[a]****	3.6 ± 0.5	5.6 ± 0.4[b]***	2.4 ± 0.1[f]**	4.3 ± 0.5[c, e]**	2.8 ± 0.2	5.2 ± 0.4[d]****
RBG (mmol/L)	8	7.1 ± 0.4	7.0 ± 0.7	6.9 ± 0.2	7.2 ± 0.3	7.1 ± 0.2	6.6 ± 0.7	5.9 ± 1.1	6.2 ± 0.7
FBG (mmol/L)	8	5.2 ± 0.3	6.1 ± 0.6	5.5 ± 0.4	4.8 ± 0.7	5.2 ± 0.4	4.4 ± 0.6	3.9 ± 1.4	4.6 ± 0.5
Fasting insulin (μIU)	6	24.9 ± 6.2	74.4 ± 12.1[a]*	20.2 ± 8.2	80.2 ± 13.9[b]*	34.8 ± 9.4	30.7 ± 7.7[e]*	24.6 ± 3.6	50.1 ± 8.1[d]*
HOMA-IR	6	4.6 ± 1.4	19.2 ± 3.6[a]*	4.5 ± 1.2	18.6 ± 3.1[b]*	8.4 ± 2.0	7.4 ± 2.1[e]*	4.4 ± 0.9	12.2 ± 2.4[d]*
CD (μmol/mmol)	6	35.7 ± 2.7	33.1 ± 2.4	31.5 ± 1.5	28.7 ± 2.6	24.5 ± 2.2[f]*	22.3 ± 2.1[e]*	20.1 ± 1.7[h]**	23.1 ± 2.5[g]***
TBARS (μmol/mmol)	6	1.5 ± 0.2	1.62 ± 0.1	1.4 ± 0.16	1.8 ± 0.3	1.8 ± 0.3	1.5 ± 0.1	1.7 ± 0.1	1.2 ± 0.1[d,g]*
TC (mmol/L)	6	2.51 ± 0.22	2.54 ± 0.16	2.44 ± 0.20	2.20 ± 0.22	2.44 ± 0.19	2.54 ± 0.24	2.61 ± 0.26	2.54 ± 0.20
TGs	6	0.62 ± 0.08	0.96 ± 0.14[a]*	0.64 ± 0.07	0.96 ± 0.12	0.74 ± 0.08	0.88 ± 0.12	0.96 ± 0.16	0.94 ± 0.08
LDL-C	5	1.8 ± 0.2	2.0 ± 0.1	1.9 ± 0.3	1.9 ± 0.2	2.2 ± 0.1	2.4 ± 0.3	1.8 ± 0.2	2.2 ± 0.3
HDL-2	6	0.11 ± 0.01	0.15 ± 0.05	0.18 ± 0.03[f]*	0.19 ± 0.04[e]*	0.07 ± 0.03	0.07 ± 0.02	0.17 ± 0.05	0.08 ± 0.02
HDL-3	5	0.24 ± 0.04	0.34 ± 0.02[a,g]*	0.29 ± 0.03	0.22 ± 0.02[i]*	0.22 ± 0.03	0.17 ± 0.02	0.19 ± 0.01[h]*	0.24 ± 0.02

Results are presented as mean ± SEM. *p < .05, **p < .01, ***p < .001, ****p < .0001.
RBG – random blood glucose, FBG – fasting blood glucose, HOMA – homeostasis model assessment for insulin resistance, CD – conjugated dienes, TBARS – thiobarbituric acid reactive substances, HCD – high-calorie diet, TC – total cholesterol, LDL-C – low-density lipoprotein cholesterol, HDL – high-density lipoprotein, TGs – triglycerides, TBM – total body mass, IP – intraperitoneal fat, AI – adiposity index. Statistical analyses: 1-way ANOVA with Bonferroni post-hoc test.

[a] HCD control vs lean control.
[b] HCD highly active antiretroviral therapy (HAART) vs lean HAART.
[c] HCD HAART + Saro (Saroglitazar) vs lean HAART + Saroglitazar.
[d] HCD Saroglitazar vs lean Saroglitazar.
[e] HCD HAART vs HCD HAART+ Saroglitazar.
[f] lean HAART vs lean HAART + Saroglitazar.
[g] HCD+ Saroglitazar vs HCD control.
[h] lean Saroglitazar vs. lean control.
[i] HCD control vs HCD HAART.

harvested and weighed (expressed as: Adiposity Index (AI) = IP fat/TBM*100).

2.2. Biochemical analyses

Blood glucose levels were measured in millimoles/litre (mmol/L) using a conventional glucometer (GlucoPlus™ Cipla MedPro (Pty) Ltd. SouthAfrica) for fasted and non-fasted animals.

Fasting insulin levels (μIU/mL) were analyzed using RayBio® rat insulin enzyme-linked immunosorbent assay kit (ELISA), (RayBiotech, Norcross, USA) as per the manufacturer's protocol. Subsequently, the homeostasis model assessment for insulin resistance (HOMA- IR), was calculated using the formula: fasting serum insulin concentration (μIU/L)*FBG (mg/dl)/405 [27]. HOMA-IR is a validated method of assessing insulin resistance and β cell function in Wistar rats [28].

2.2.1. Markers of lipid peroxidation

Conjugated dienes (CD) concentrations (μmol/L) were calculated at absorbance of 234 nm following cyclohexane dilution as previously described [29,30]. Thiobarbituric acid reactive substances (TBARS) concentrations (μmol/L) were determined with spectrophotometry at an absorbance of 532 nm after addition of thiobarbituric acid reagent (Sigma-Aldrich, USA) to a mixture of butylated hydroxytoluene (Fluka Chemie-Switzerland), ethanol (Merck, SA) and orthophosphoric acid (Sigma-Aldrich, USA) [31].

2.2.2. Lipid analysis

High-density lipoprotein cholesterol (HDL−C) and its subclasses HDL2 and HDL3 (μmol/L) concentrations were analyzed as per a previously published protocol [32]. Serum total cholesterol (TC) and triglyceride (TG) concentrations (mmol/L) were assessed using enzymatic colorimetric kits (LabAssay™ Cholesterol (catalogue number 294–65801), LabAssay™ TG (catalogue number 290–63701), using a SPECTRA-max Plus 384 spectrophotometer with SoftMax Pro 4.8 microplate data acquisition and analysis software (Molecular Devices Corporation, Labotec Industrial Technologies, South Africa).

See supplementary methods (supplementary material 1) for a more detailed description of the biochemical analyses.

2.3. Western blot analyses

Standard Western blot techniques were employed, as described previously [33], to measure proteins of interest, i.e. (i) proteins involved in vascular homeostasis, cytoprotection and inflammatory/stress response: - adenosine monophosphate activated protein kinase (AMPK), inhibitor of kappa B alpha (IκBα), protein kinase B (PKB/Akt); peroxisome proliferator-activated receptor gamma coactivator 1-alpha (PGC-1α), and mitogen-activated protein kinases (MAPK), JNK, Erk1/2 and p38 MAPK (ii) vascular tone regulatory protein: endothelial nitric oxide synthase (eNOS); iii) apoptosis: cleaved poly (ADP-ribose) polymerase (PARP) and caspase 3; (iv) endothelial oxidative stress nicotinamide adenine dinucleotide phosphate (NADPH) subunit, p22-phox. (see Table, supplementary material 2, demonstrating Western blot protocol/antibodies).

2.4. Aortic ring isometric tension studies

Isolated aortic ring isometric tension output was recorded on LabChart® 7 data acquisition and analysis software (Dunedin, New Zealand) as per previously published protocols [33,34]. Measurement of vasorelaxation following acetylcholine stimulation is considered the gold standard technique for the evaluation of endothelium-dependent vasodilation [35] (see Figure, supplementary material 3, illustrating aortic ring isometric tension protocol).

2.5. Statistical analyses

Values are expressed as mean ± standard error of the mean (SEM); for multiple group comparisons, one-way analysis of variance (ANOVA) was used (GraphPad Prism® Plus Version 6.0) followed by Bonferroni's post-hoc test, $p < .05$ was considered statistically significant. Vascular reactivity data were analyzed by two-way ANOVA and Bonferroni's post-hoc test. The EC_{50} (the drug concentration inducing 50% of the maximal response), was determined by nonlinear regression model analysis following the log X (dose) vs. response transformation of the percentage relaxation or tension.

3. Results

3.1. Biometric measurements and biochemical analyses

Before onset of HAART, HCD induced higher TBM compared to control diet (week 10, Table 1). Following treatment, the HCD-fed animals continued to register higher TBM compared to their chow-fed counterparts. However, no additional changes in TBM were ascribed to the various treatments (Table 1). Similarly, the AI was significantly higher in HCD compared to chow-fed animals. Interestingly, Saroglitazar co-treatment with HAART significantly reduced the AI in both chow-fed and HCD-fed animals vs. HAART only-treated groups. Although no significant differences were observed in the mean random blood glucose (RBG) and fasting blood glucose (FBG) levels among the experimental groups, of importance to note is that when Saroglitazar was administered in obese animals on HAART, the mean fasting serum insulin and CD significantly decreased compared to the HAART only-treated counterparts. Mean HOMA-IR followed similar trends. Saroglitazar monotherapy significantly reduced fasting insulin and HOMA-IR in the HCD animals compared to the lean ones (Table 1).

No significant changes were observed in serum TC and LDL-C levels. However, TG and HDL-3 levels were significantly higher in untreated obese animals compared to their lean control counterparts. Both Saroglitazar and HAART-treated obese animals had lower HDL-3 levels compared to the obese controls. Similarly, Saroglitazar-treated obese animals registered lower TBARS levels compared to both untreated lean and obese controls (Table 1).

3.2. Aortic ring isometric tension studies

3.2.1. Phenylephrine-induced aortic contraction

The maximal mean tension (E_{max}) following phenylephrine administration was significantly higher in the lean animals treated with Saroglitazar compared to untreated and HAART-exposed lean animals. No significant differences were observed in the mean log EC_{50}

Table 2
Phenylephrine-induced maximal aortic contraction (Emax) and Log EC_{50}.

Experimental group	n/group	Phenylephrine-induced contraction	
		Mean ± SEM E_{max} Tension (g)	Mean ± SEM (Log EC_{50})
Lean Control	9	2.1 ± 0.1	0.84 ± 0.75
HCD Control	8	2.2 ± 0.2	0.83 ± 0.60
Lean HAART	9	2.0 ± 0.2	0.96 ± 0.71
HCD HAART	9	2.3 ± 0.2	0.52 ± 0.38
Lean HAART + Saro	8	2.2 ± 0.2	0.68 ± 0.49
HCD HAART + Saro	8	2.1 ± 0.2	0.84 ± 0.45
Lean Saro	8	2.5 ± 0.2**	0.92 ± 0.83
HCD Saro	8	2.3 ± 0.2	0.80 ± 0.31

**$p < .01$; lean Saro (Saroglitazar) group vs. lean control group and lean highly active antiretroviral therapy (HAART) group. HCD – high-calorie diet, E_{max} – maximum tension. Statistical analyses: 2-way ANOVA with Bonferroni post-hoc test.

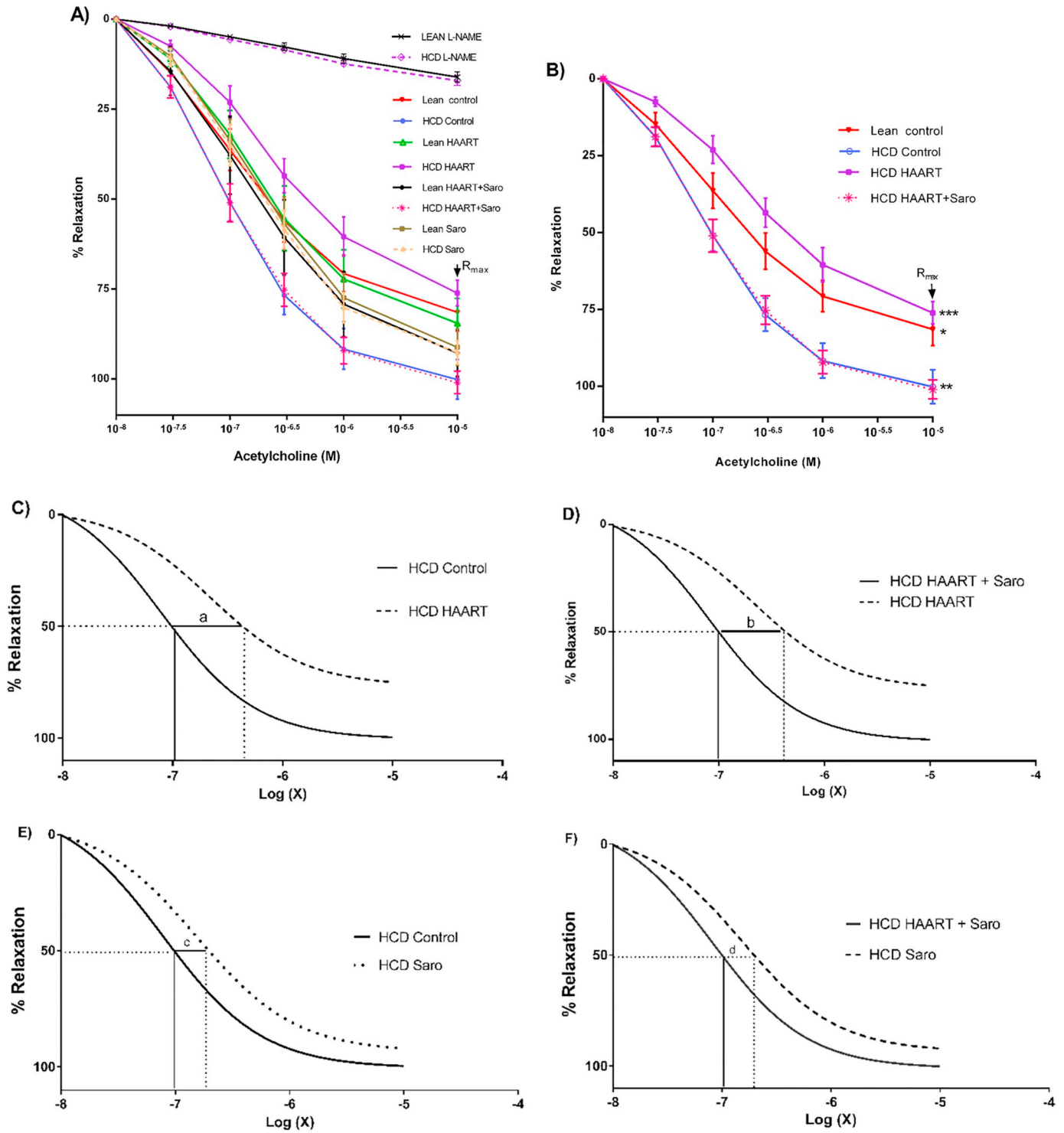

Fig. 1. Acetylcholine-induced aortic relaxation curves. A: Acetylcholine dose-induced aortic response for all the experimental groups, including demonstration of NO synthase involvement with L-NAME pre-treatment. B: Acetylcholine dose-induced aortic response showing groups with significant differences in the R_{max}. ***$p < .001$ (HCD HAART + Saroglitazar vs. HCD HAART); **$p < .01$ (HCD control vs. HCD HAART); *$p < .05$ (HCD control vs. lean control). C-F: Nonlinear regression (curve fit) of log transformed acetylcholine-induced aortic relaxation, EC_{50}. C: HCD control vs. HCD HAART, $^{a}p = 0.003$; D: HCD + HAART vs. HCD HAART + Saroglitazar, $^{b}p = 0.002$; E: HCD control vs. HCD + Saroglitazar, $^{c}p = 0.03$; F: HCD HAART + Saroglitazar vs. HCD Saroglitazar, $^{d}p = 0.024$. $n = 8–9$/group. L-NAME - L-nitroarginine methyl ester, HCD – high-calorie diet, HAART – highly active antiretroviral therapy, Saro – Saroglitazar. Statistical analyses: 2-way ANOVA with Bonferroni post-hoc test.

(Table 2).

3.2.2. Acetylcholine-induced aortic relaxation

The curves (Fig. 1A) represent mean percentage relaxation of the aortic rings (per group) from phenylephrine E_{max} to the maximum relaxation (R_{max}) achieved following cumulative doses of acetylcholine. L-nitroarginine methyl ester (L-NAME) administration attenuated acetylcholine-mediated relaxation in both lean and HCD groups

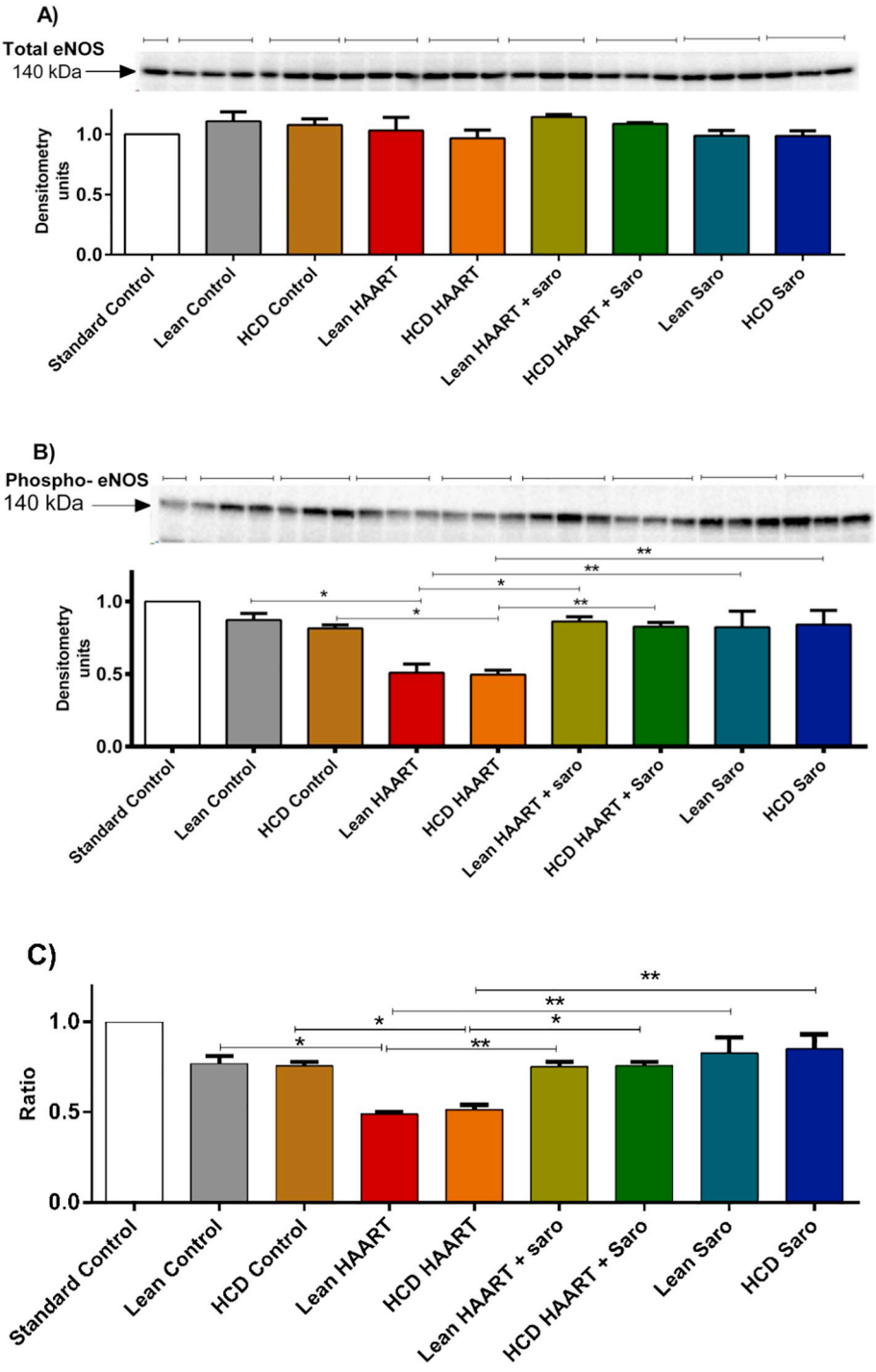

Fig. 2. Western blot measurements of aortic eNOS and PKB/Akt expression and phosphorylation. A: total eNOS expression; B: phosphorylated (phospho)-eNOS measurements; C: phospho-eNOS: total eNOS ratio. D: Total PKB/Akt expression; E: phospho-PKB/Akt; F: phospho-PKB/Akt: total PKB/Akt ratio. Standard control: sample prepared from untreated rats for normalization. $*p < .05$; $**p < .01$; $***p < .001$, $n = 3$/group. Statistical analyses: 1-way ANOVA with Bonferroni post-hoc test.

(Fig. 1A). HAART exposure in obese animals induced a significant reduction in R_{max} compared to the untreated obese animals. Interestingly, co-treatment of obese animals with HAART + Saroglitazar significantly improved the R_{max} compared to obese HAART-treated animals. Untreated obese animals recorded a significantly higher R_{max} compared to the standard rat chow-fed animals (Fig. 1B).

The EC_{50} for the obese animals treated with HAART was significantly higher compared to that of non-treated obese animals (Fig. 1C). However, following co-treatment of the obese animals with HAART and Saroglitazar, the EC_{50} was significantly improved compared to HAART only-treated obese animals (Fig. 1D). Similarly, Saroglitazar monotherapy induced a poorer response compared to untreated and HAART + Saroglitazar obese groups (Fig. 1E and Fig. 1F, respectively).

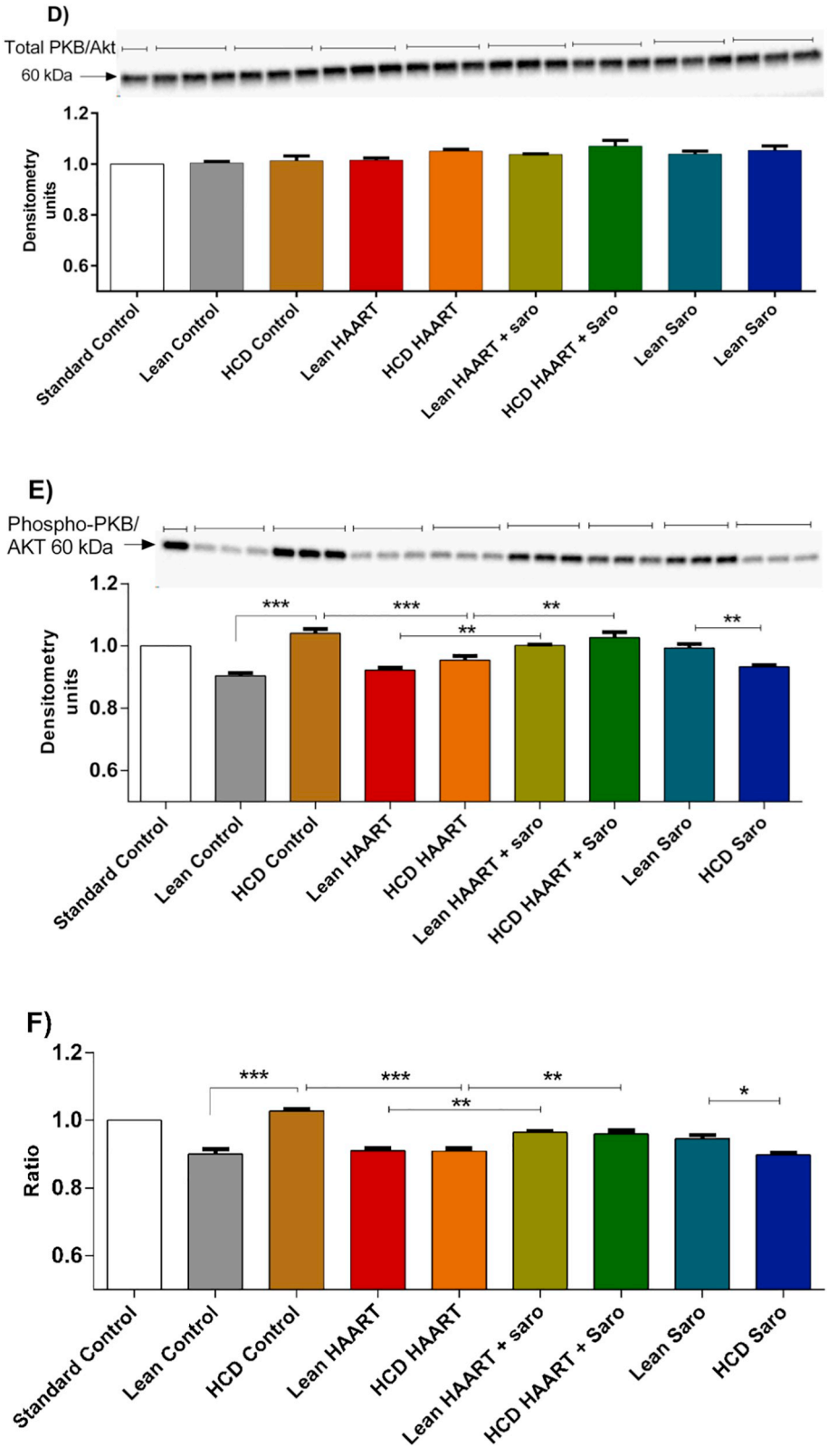

Fig. 2. (*continued*)

3.3. Aortic tissue protein determination: western blot results

3.3.1. Endothelial nitric oxide synthase (eNOS)

No significant differences were observed in total eNOS expression (Fig. 2A). However, HAART downregulated eNOS activity in both lean and HCD animals as evidenced by lower phospho-eNOS levels and phospho-eNOS: total eNOS ratios compared to their respective untreated counterparts. On the other hand, Saroglitazar monotherapy and HAART + Saroglitazar upregulated the phosphorylation of eNOS compared to HAART only treatment in both lean and obese animals (Fig. 2B and C).

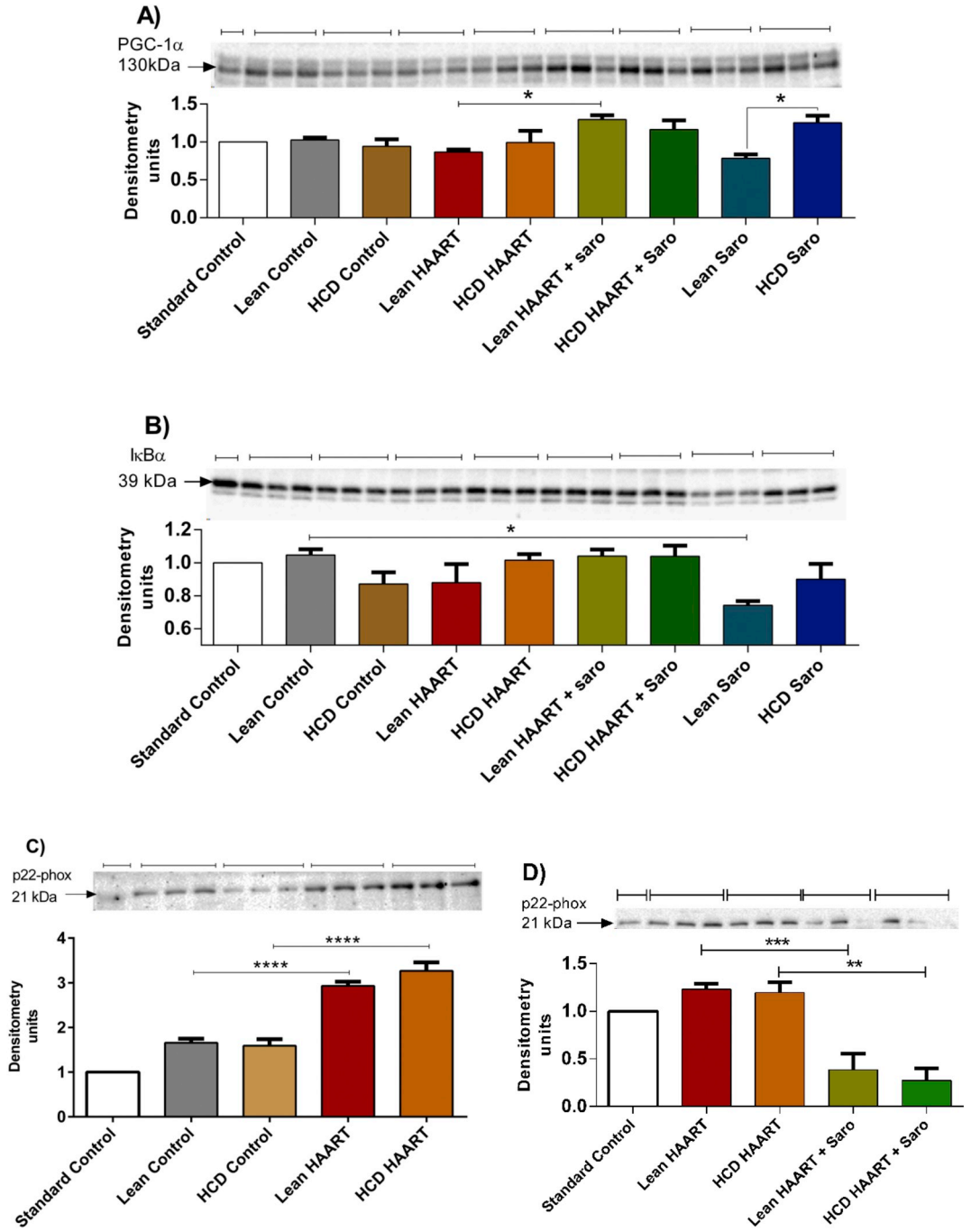

Fig. 3. Western blot measurements of aortic PGC-1α, IκBα and p22-phox expression. A: Peroxisome proliferator-activated receptor gamma coactivator 1-alpha (PGC-1α) expression. B: Inhibitor of kappa B alpha (IκBα) expression. C, D: Nicotinamide adenine dinucleotide phosphate subunit, p22-phox expression. *$p < .05$; **$p < .01$; ***$p < .001$, ****$p < .0001$; $n = 3$/group. Statistical analysis: 1-way ANOVA with Bonferroni post-hoc test.

3.3.2. PKB/Akt

Total PKB/Akt expression remained unaltered (Fig. 2D). However, phospho-PKB/Akt levels were significantly higher in the untreated obese animals compared to the lean control animals. HAART significantly downregulated the phosphorylation of PKB/Akt in obese animals compared to their untreated counterparts (Fig. 2E). Interestingly, co-administration of Saroglitazar in HAART-treated lean and obese animals, significantly upregulated the phosphorylation of PKB/Akt compared to HAART only-treated counterparts. Unexpectedly, Saroglitazar monotherapy downregulated phospho-PKB/Akt levels in obese animals compared to the lean counterparts (Fig. 2E). Phospho: total ratio of PKB/Akt followed similar trends (Fig. 2F).

3.3.3. PGC-1α and IκBα

PGC-1α expression levels were significantly higher in the lean animals treated with HAART + Saroglitazar compared to the lean animals treated with HAART only. Similarly, Saroglitazar monotherapy significantly upregulated PGC-1α levels in HCD animals compared to their lean counterparts. No other significant differences were observed (Fig. 3A). IκBα expression was only downregulated in lean animals treated with Saroglitazar compared to the lean control animals (Fig. 3B).

3.3.4. p22-phox

HAART exposure significantly upregulated the expression of aortic

p22-phox in both lean and obese animals compared to their control counterparts (Fig. 3C). Interestingly, the aortic p22-phox expression was significantly downregulated in both lean and obese animals receiving HAART in combination with Saroglitazar compared to their HAART-only treated counterparts (Fig. 3D).

No significant differences were observed in the aortic expression of AMPK, cleaved caspase-3 and cleaved PARP. Similarly, aortic MAPKs and PPARα/γ expression were unaltered (see supplementary results, Figs. 1–5).

4. Discussion

In the present study, HCD-induced obese rats were treated for a period of 6 weeks with a common PI-based HAART regimen and a dual PPARα/γ agonist. Although we did not measure the plasma drug concentrations achieved, a previous study clearly demonstrated that younger, male Sprague-Dawley rats when treated with even lower doses of NRTI (AZT) and a PI, (indinavir) (monotherapy or in combination) achieved efficacious steady-state concentrations comparable to those measured in humans [13]. We further evaluated the role of these drugs in the context of metabolic and vascular changes. Our findings clearly demonstrate that HAART-exposed obese rats progressively manifested with increased TBM, increased AI, insulin resistance and the development of endothelial dysfunction. However, these characteristics were attenuated following Saroglitazar co-treatment with HAART in obese animals.

Current trends indicate that non-AIDS-related cardiometabolic events are emerging as a major health burden in HIV-infected populations [36]. The pathophysiological mechanisms underlying these events are still incompletely understood because specific organ disturbances are multifactorial in aetiology. For example, HAART may in itself exacerbate the chronic effects of HIV exposure which is now considered an independent risk factor in the development of non-communicable diseases such as obesity, CVD and T2DM [37]. In addition, increased BMI and abdominal circumference are associated with increased risk of CVD and T2DM in HIV patients receiving HAART [38]. This finding has been replicated in a mouse model of high fat diet (58.0 kcal% fat) treated with efavirenz, emtricitabine, and tenofovir for 12 weeks (commenced simultaneously with the diet) where, the HAART regimen not only led to increased fat mass, but also induced impaired glucose tolerance, potentiated insulin resistance and was associated with increased adipocyte inflammation [39]. In the present study, differences in rat TBM and AI were only ascribed to consumption of obesogenic diet but not with exposure to a combination of PIs and NRTIs. Therefore, the six-weeks' HAART regimen did not additionally alter obesity status compared to the untreated control counterparts. However, in a novel finding, our study showed that following dual PPARα/γ agonist coadministration with HAART, the AI was significantly reduced in both lean and obese animals despite no notable significant differences in blood glucose, TC, TGs, and LDL-C levels (Table 1).

Although Saroglitazar has previously been investigated in HIV-infected patients receiving HAART [24], TBM changes were undocumented. However, 12-weeks of Saroglitazar therapy in HIV-infected patients with dyslipidemia increased the HDL-C levels and reduced TGs, VLDL, and TC [24]. Our findings did not reveal changes in the TC, TGs or LDL following HAART, with/without Saroglitazar exposure, which may be due to an insufficient treatment duration. However, in contrast to the findings of Deshpande et al., [24] on fasting insulin levels (elevated fasting insulin and elevated HOMA-IR in Saroglitazar-treated patients), our data showed that HAART induced an increase in fasting insulin levels and HOMA-IR index and Saroglitazar significantly reduced HOMA-IR and fasting insulin in obese rats treated with HAART (Table 1).

Stimulation of PPARα/γ has been employed in obesity and T2DM therapy to improve insulin resistance and thereby regulate the accompanying dyslipidemia and hyperglycemia. For example, the thiazolidinedione, rosiglitazone (PPARγ agonist), has been shown to improve lipid and glucose profiles in obese, insulin-resistant rats [40]. The PPARγ receptors are predominantly expressed in adipose tissue and their stimulation has been implicated in gene regulation leading to adipocyte differentiation and adipocytokine regulation [41]. Lipid activated transcriptional factor PPARα (a potent lipoprotein/fatty acid metabolism regulator), stimulation attenuates dyslipidemia and insulin resistance [42]. Despite observing no alterations in the lipid profiles of the HAART-treated obese animals in the current study, dual stimulation of PPARα/γ improved insulin resistance, fasting insulin and CD (Table 1). The HDL-2/3 levels were, however, reduced by Saroglitazar in HAART-exposed obese animals. Although previous studies only reported an increase in HDL-C without interrogating further the HDL subclasses [24,42], the HCD in the present study increased the HDL-3 subtype with no significant changes in TC (Table 1). Further investigations to fully elucidate this implication ought to be conducted, since cardioprotective antioxidant enzymes and sphingosine-1-phosphate are linked to HDL-3 subtype [43].

Our findings clearly demonstrate that endothelium-mediated vasorelaxation was impaired by HAART administration in obese animals despite no changes in contractility (Table 2 and Fig. 1A, B). Similarly, protective signaling proteins associated with endothelial homeostasis were downregulated in HAART-exposed obese rats as evidenced by downregulation of phosphorylated eNOS and PKB/Akt levels (Fig. 2). Upregulation of phospho-PKB/Akt in untreated obese animals was also associated with increased vasorelaxation compared to control animals. PKB/Akt in the vascular tissue plays a critical role in the maintenance of homeostasis and angiogenesis regulating many vascular processes such as cell migration, glucose metabolism, protein synthesis, cell attachment, survival and nitric oxide (NO) production [44]. Downregulation of phospho-eNOS in obese rat aortas receiving HAART may explain impairment of aortic relaxation, since acetylcholine-induced endothelium-dependent relaxation is mediated via muscarinic receptor binding and concomitant production of NO that results in vascular smooth muscle relaxation [45]. Other deleterious effects of impaired eNOS signaling include, susceptibility to coagulation/thrombosis and atherogenicity and thereby overall increased cardiovascular risk [46].

HAART exposure in obese animals was associated with increased vascular oxidative stress as evidenced by upregulation of p22-phox (Fig. 3C). Chronic antiretroviral therapy has previously been associated with oxidative stress [47] but the link to endothelial dysfunction in HAART remains unclear [13]. In addition to upregulation of aortic p22-phox expression, obese animals treated with HAART also had elevated levels of CD (Table 1) despite no changes in TBARS levels. All these factors have previously been associated with poor endothelial function and increased cardiovascular risk in HIV-infected patients [48].

The pro-atherogenic milieu in patients treated with PIs is characterised by demonstrable increased carotid intima media thickness and atherosclerosis associated with myocardial infarction [37]. NRTIs induce mitochondrial dysregulation that ultimately leads to endothelial cell and cardiac cell dysfunction as a result of mitochondrial polymerase-γ inhibition and increased oxidative stress [49]. These effects are not only limited to endothelial/cardiac cells, but also affect other organs such as the liver leading to hepatotoxicity [50].

The endothelium is key in regulation of vascular tone, inflammation, platelet function and hemostasis [51] and is highly susceptible to the deleterious effects of various compounds either endogenously secreted or exogenously administered. For example, antiretroviral agents increase susceptibility to endothelial damage and subsequent development of CVD in HIV-infected patients [52]. Although previously it was thought that endothelial dysfunction and increased cardiovascular risk in HAART resulted from PI-induced dyslipidemia and atherosclerosis [37], there is emerging evidence suggesting that these drugs may, in fact, cause direct endothelial dysfunction in vivo [13]. In addition, direct effects of NRTIs on cardiac mitochondrial bioenergetics have been reported [53].

In the present study, Saroglitazar demonstrated the potential to ameliorate HAART-induced vascular dysfunction in obese rats. The acetylcholine-induced endothelium-dependent vasorelaxation was improved in combined therapy (Fig. 1), as well as upregulation of eNOS and PKB/Akt signaling cascades in HCD despite unaltered aortic MAPK and PPARα/γ expression (supplementary results Figs. 1–5). Similarly, Saroglitazar downregulated the pro-oxidative stress marker of NADPH-oxidase, p22-phox, as well as serum CD levels. Our findings support previous studies that demonstrate that PPARα activation protects T2DM myocardium against ischemia-reperfusion through phosphoinositide 3-kinase/Akt and NO pathway [54]. We therefore postulate that dual PPARα/γ-mediated correction of insulin resistance, upregulation of protective aortic signaling pathways (PKB/Akt and eNOS), and downregulation of pro-oxidative stress NADPH-oxidase activity (p22-phox) in the aortas of HCD rats receiving HAART, may be a possible mechanism underlying the functional amelioration of HAART-induced vascular dysfunction in these animals.

5. Conclusion

In the present study, exposure of HCD-induced obese rats to HAART resulted in aortic endothelial dysfunction, possibly as a result of the development of insulin resistance, and direct impairment of aortic PKB/Akt and eNOS signaling accompanied by upregulation of pro-oxidative NADPH-oxidase activity. In a novel finding, we have shown that co-treatment with a dual PPARα/γ agonist conferred protection against the HAART-induced endothelial dysfunction through the abolishment of insulin resistance, upregulation of the PKB/Akt and eNOS signaling proteins, and downregulation of NADPH-oxidase activity. These results point to a harmful pro-endothelial dysfunction role for HAART in the presence of obesity, and a potential role for dual PPARα/γ stimulation as a therapeutic option in mitigating the harmful effects of HAART. The findings are relevant in view of the additional cardiovascular risk posed by rising obesity rates in HIV-infected populations and increasing global access to HAART.

5.1. Study limitations

Our animal model was devoid of HI-Viral antigens and proteins, and future studies should incorporate humanized HI-Viral animal models (e.g. transgenic mice) since these proteins are implicated in endothelial damage. The aorta represents the conduit type of arterial vessels and therefore further studies on the resistance type of arterial network are recommended. Although outside the scope of the present study, biomarkers of vascular dysfunction such as the expression of adhesion molecules and endothelin-1, as well as pro-inflammatory cytokines, were not investigated, these would have provided important additional insights and strengthened the conclusions of the present study. Future studies using in vitro endothelial cell models should be considered for such investigations.

Acknowledgements

The authors are grateful to the Faculty of Medicine and Health Sciences, Stellenbosch University, and the South African Medical Research Council (SAMRC), Biomedical Research and Innovation Platform (BRIP) for research funding and logistical support.

Conflicts of interest and source of funding

For all the authors, none were declared.

Meetings at which parts of the data were presented.

Conference: 44th Conference of the Physiology Society of Southern Africa (PSSA), Cape Town, South Africa. 28–31 August 2016.

Conference: First Conference of Biomedical and Natural Sciences and Therapeutics (CoBNest), Stellenbosch, South Africa. 7–10 October 2018.

Conference: 4th EU-SA (SASCAR) Cardiovascular Research workshop STIAS, Stellenbosch, South Africa. 1-4th April 2019.

Funding

This work was supported by Faculty of Medicine and Health Sciences, Stellenbosch University and South African Medical Research Council (SAMRC), Biomedical Research and Innovation Platform (BRIP).

Appendix A. Supplementary data

Supplementary data to this article can be found online at https://doi.org/10.1016/j.vph.2019.106577.

References

[1] J.A.C. Sterne, M.A. Hernán, B. Ledergerber, K. Tilling, R. Weber, P. Sendi, et al., S.H.I.V.C. Study, Long-term effectiveness of potent antiretroviral therapy in preventing AIDS and death: a prospective cohort study, Lancet 366 (2005) 378–384.

[2] E. Sezgin, M.L. Van Natta, J.E. Thorne, M.A. Puhan, D.A. Jabs, L.S. of the O.C. of A. (SOCA) R. Group, Secular trends in opportunistic infections, cancers and mortality in patients with AIDS during the era of modern combination antiretroviral therapy, HIV Med. 19 (2018) 411–419.

[3] L.F. Johnson, J. Mossong, R.E. Dorrington, M. Schomaker, C.J. Hoffmann, O. Keiser, et al., Life expectancies of South African adults starting antiretroviral treatment: collaborative analysis of cohort studies, PLoS Med. 10 (2013) e1001418.

[4] D.E. Vance, M. Mugavero, J. Willig, J.L. Raper, M.S. Saag, Aging with HIV: a cross-sectional study of comorbidity prevalence and clinical characteristics across decades of life, J. Assoc. Nurses AIDS Care. 22 (2011) 17–25.

[5] C. Vigouroux, S. Gharakhanian, Y. Salhi, T.H. Nguyen, N. Adda, W. Rozenbaum, et al., Adverse metabolic disorders during highly active antiretroviral treatments (HAART) of HIV disease, Diabetes Metab. 25 (1999) 383–392.

[6] S. Grinspoon, A. Carr, Cardiovascular risk and body-fat abnormalities in HIV-infected adults, N. Engl. J. Med. 352 (2005) 48–62.

[7] H.R. Zanetti, E.L. Mendes, A.C.P. Chagas, M.O.G. Douglas, L.T.P. Lopes, L. Roever, et al., Triad of the ischemic cardiovascular disease in people living with HIV? Association between risk factors, HIV infection, and use of antiretroviral therapy, Curr. Atheroscler. Rep. 20 (2018) 30.

[8] V. Amorosa, M. Synnestvedt, R. Gross, H. Friedman, R.R. MacGregor, D. Gudonis, et al., A tale of 2 epidemics: the intersection between obesity and HIV infection in Philadelphia, J. Acquir. Immune Defic. Syndr. 39 (2005) 557–561 http://www.ncbi.nlm.nih.gov/pubmed/16044007.

[9] N. Crum-Cianflone, M.P. Roediger, L. Eberly, M. Headd, V. Marconi, A. Ganesan, et al., Increasing rates of obesity among HIV-infected persons during the HIV epidemic, PLoS One 5 (2010) 1–9, https://doi.org/10.1371/journal.pone.0010106.

[10] M. Gelpi, S. Afzal, J. Lundgren, A. Ronit, A. Roen, A. Mocroft, et al., Higher risk of abdominal obesity, elevated LDL cholesterol and hypertriglyceridemia, but not of hypertension, in people living with HIV: results from the Copenhagen comorbidity in HIV infection (COCOMO) study, Clin. Infect. Dis. 67 (2018) 579–586.

[11] J.C. Price, E.C. Seaberg, R. Latanich, M.J. Budoff, L.A. Kingsley, F.J. Palella, et al., Risk factors for fatty liver in the multicenter AIDS cohort study, Am. J. Gastroenterol. 109 (2014) 695–704, https://doi.org/10.1038/ajg.2014.32.

[12] D. Francisci, S. Giannini, F. Baldelli, M. Leone, B. Belfiori, G. Guglielmini, et al., HIV type 1 infection, and not short-term HAART, induces endothelial dysfunction, AIDS 23 (2009) 589–596.

[13] B. Jiang, V.Y. Hebert, J.H. Zavecz, T.R. Dugas, Antiretrovirals induce direct endothelial dysfunction in vivo, JAIDS J. Acquir. Immune Defic. Syndr. 42 (2006) 391–395.

[14] B. Jiang, V.Y. Hebert, Y. Li, J.M. Mathis, J.S. Alexander, T.R. Dugas, HIV antiretroviral drug combination induces endothelial mitochondrial dysfunction and reactive oxygen species production, but not apoptosis, Toxicol. Appl. Pharmacol. 224 (2007) 60–71.

[15] R. Chetty, Vasculitides associated with HIV infection, J. Clin. Pathol. 54 (2001) 275–278, https://doi.org/10.1136/jcp.54.4.275.

[16] F.J. Torriani, L. Komarow, R.A. Parker, B.R. Cotter, J.S. Currier, M.P. Dubé, et al., Endothelial function in human immunodeficiency virus-infected antiretroviral-naive subjects before and after starting potent antiretroviral therapy: the ACTG (AIDS Clinical Trials Group) Study 5152s, J. Am. Coll. Cardiol. 52 (2008) 569–576.

[17] J.H. Stein, M.A. Klein, J.L. Bellehumeur, P.E. McBride, D.A. Wiebe, J.D. Otvos, et al., Use of human immunodeficiency virus-1 protease inhibitors is associated with atherogenic lipoprotein changes and endothelial dysfunction, Circulation 104 (2001) 257–262.

[18] X. Wang, H. Chai, Q. Yao, C. Chen, Molecular mechanisms of HIV protease inhibitor-induced endothelial dysfunction, JAIDS J. Acquir. Immune Defic. Syndr. 44 (2007) 493–499.

[19] A.R. Eckard, Y. Jiang, S.M. Debanne, N.T. Funderburg, G.A. McComsey, Effect of 24 weeks of statin therapy on systemic and vascular inflammation in HIV-infected subjects receiving antiretroviral therapy, J. Infect. Dis. 209 (2014) 1156–1164.

[20] G.M. Ray, Antiretroviral and statin drug-drug interactions, Cardiol. Rev. 17 (2009) 44–47.
[21] E. Negredo, J. Molto, J. Puig, D. Cinquegrana, A. Bonjoch, N. Perez-Alvarez, et al., Ezetimibe, a promising lipid-lowering agent for the treatment of dyslipidaemia in HIV-infected patients with poor response to statins, AIDS 20 (2006) 2159–2164.
[22] S. Bellosta, A. Corsini, Statin drug interactions and related adverse reactions: an update, Expert Opin. Drug Saf. 17 (2018) 25–37.
[23] R. Agrawal, The first approved agent in the Glitazar's class: saroglitazar, Curr. Drug Targets 15 (2014) 151–155.
[24] A. Deshpande, H. Toshniwal, S. Joshi, R.H. Jani, A prospective, multicentre, open-label single-arm exploratory study to evaluate efficacy and safety of saroglitazar on hypertriglyceridemia in HIV associated lipodystrophy, PLoS One 11 (2016) 1–12, https://doi.org/10.1371/journal.pone.0146222.
[25] L.C. Pickavance, M. Tadayyon, P.S. Widdowson, R.E. Buckingham, J.P.H. Wilding, Therapeutic index for rosiglitazone in dietary obese rats: separation of efficacy and haemodilution, Br. J. Pharmacol. 128 (1999) 1570–1576.
[26] A.B. Nair, S. Jacob, A simple practice guide for dose conversion between animals and human, J. Basic Clin. Pharm. 7 (2016) 27–31, https://doi.org/10.4103/0976-0105.177703.
[27] D.R. Matthews, J.P. Hosker, A.S. Rudenski, B.A. Naylor, D.F. Treacher, R.C. Turner, Homeostasis model assessment: insulin resistance and β-cell function from fasting plasma glucose and insulin concentrations in man, Diabetologia 28 (1985) 412–419.
[28] L.C. Antunes, J.L. Elkfury, M.N. Jornada, K.C. Foletto, M.C. Bertoluci, Validation of HOMA-IR in a Model of Insulin-Resistance Induced by a High-Fat Diet in Wistar Rats 1, 60 (2016), pp. 138–142, https://doi.org/10.1590/2359-3997000000169.
[29] H. Esterbauer, G. Striegl, H. Puhl, M. Rotheneder, Continuous monitoring of in vztro oxidation of human low density lipoprotein, Free Radic. Res. Commun. 6 (1989) 67–75.
[30] W.A. Pryor, L. Castle, [34] chemical methods for the detection of lipid hydroperoxides, in: Methods Enzymol. (ISSN: 0076-6879, vol. 105, Issue: C, Page: 293–299). https://doi.org/10.1016/S0076-6879(84)05037-0
[31] A.M. Jentzsch, H. Bachmann, P. Fürst, H.K. Biesalski, Improved analysis of malondialdehyde in human body fluids, Free Radic. Biol. Med. 20 (1996) 251–256.
[32] L.I. Gidez, G.J. Miller, M. Burstein, S. Slagle, H.A. Eder, Separation and quantitation of subclasses of human plasma high density lipoproteins by a simple precipitation procedure, J. Lipid Res. 23 (1982) 1206–1223.
[33] C. Westcott, A. Genis, M. Mthethwa, R. Graham, D. Van Vuuren, B. Huisamen, et al., Fenofibrate protects endothelial cells against the harmful effects of TNF-alpha, SA Hear 14 (2017) 22–34, https://doi.org/10.24170/14-1-1865.
[34] B. Jespersen, N.R. Tykocki, S.W. Watts, P.J. Cobbett, Measurement of smooth muscle function in the isolated tissue bath-applications to pharmacology research, J. Vis. Exp. (2015) 52324, , https://doi.org/10.3791/52324.
[35] P.O. Bonetti, L.O. Lerman, A. Lerman, Endothelial dysfunction: a marker of atherosclerotic risk, Arterioscler. Thromb. Vasc. Biol. 23 (2003) 168–175.
[36] Cascade Collaboration, Survival after introduction of HAART in people with known duration of HIV-1 infection, Lancet 355 (2000) 1158–1159.
[37] D.C. Rhew, M. Bernal, D. Aguilar, U. Iloeje, M.B. Goetz, Association between protease inhibitor use and increased cardiovascular risk in patients infected with human immunodeficiency virus: a systematic review, Clin. Infect. Dis. 37 (2003) 959–972.
[38] A.C. Achhra, C. Sabin, L. Ryom, C. Hatleberg, M.A. d'Aminio, S. de Wit, et al., Body mass index and the risk of serious non-AIDS events and all-cause mortality in treated HIV-positive individuals: DAD cohort analysis, JAIDS J. Acquir. Immune Defic. Syndr. 78 (2018) 579–588.
[39] M.E. Pepin, L.E. Padgett, R.E. McDowell, A.R. Burg, M.K. Brahma, C. Holleman, et al., Antiretroviral therapy potentiates high-fat diet induced obesity and glucose intolerance, Mol. Metab. 12 (2018) 48–61.
[40] K.A. Imam, I. Yousaf, S. Waqas, Effect of thiazolidinediones on adipocytokines and lipid profile in insulin resistant sprague dawley rats, Pakistan, J. Physiol. 13 (2017) 3–6 http://pjp.pps.org.pk/index.php/PJP/article/view/297.
[41] T.M. Willson, J.E. Cobb, D.J. Cowan, R.W. Wiethe, I.D. Correa, S.R. Prakash, et al., The structure− activity relationship between peroxisome proliferator-activated receptor γ agonism and the antihyperglycemic activity of thiazolidinediones, J. Med. Chem. 39 (1996) 665–668.
[42] J.-M. Ye, P.J. Doyle, M.A. Iglesias, D.G. Watson, G.J. Cooney, E.W. Kraegen, Peroxisome proliferator—activated receptor (PPAR)-α activation lowers muscle lipids and improves insulin sensitivity in high fat—fed rats: comparison with PPAR-γ activation, Diabetes 50 (2001) 411–417.
[43] N.J. Woudberg, J.H. Goedecke, S. Lecour, Protection from cardiovascular disease due to increased high-density lipoprotein cholesterol in African black populations: myth or reality? Ethn. Dis. 26 (2016) 553–560.
[44] I. Shiojima, K. Walsh, Role of Akt signaling in vascular homeostasis and angiogenesis, Circ. Res. 90 (2002) 1243–1250.
[45] H.H. Knispel, C. Goessl, R. Beckmann, Basal and acetylcholine-stimulated nitric oxide formation mediates relaxation of rabbit cavernous smooth muscle, J. Urol. 146 (1991) 1429–1433.
[46] J. Qian, D. Fulton, Post-translational regulation of endothelial nitric oxide synthase in vascular endothelium, Front. Physiol. (2013) 1–11, https://doi.org/10.3389/fphys.2013.00347.
[47] B. Sharma, Oxidative stress in HIV patients receiving antiretroviral therapy, Curr. HIV Res. 12 (2014) 13–21.
[48] M. Masiá, S. Padilla, E. Bernal, M.V. Almenar, J. Molina, I. Hernández, et al., Influence of antiretroviral therapy on oxidative stress and cardiovascular risk: a prospective cross-sectional study in HIV-infected patients, Clin. Ther. 29 (2007) 1448–1455.
[49] R.L. Smith, J.M.E. Tan, M.J. Jonker, A. Jongejan, T. Buissink, S. Veldhuijzen, et al., Beyond the polymerase-γ theory: production of ROS as a mode of NRTI-induced mitochondrial toxicity, PLoS One 12 (2017) e0187424.
[50] B.H. McGovern, J.S. Ditelberg, L.E. Taylor, R.T. Gandhi, K.A. Christopoulos, S. Chapman, et al., Hepatic steatosis is associated with fibrosis, nucleoside analogue use, and hepatitis C virus genotype 3 infection in HIV-seropositive patients, Clin. Infect. Dis. 43 (2006) 365–372, https://doi.org/10.1086/505495.
[51] J. Folkman, Angiogenesis in cancer, vascular, rheumatoid and other disease, Nat. Med. 1 (1995) 27–30, https://doi.org/10.1038/nm0195-27.
[52] M. Mosepele, T. Mohammed, L. Mupfumi, S. Moyo, K. Bennett, S. Lockman, et al., HIV disease is associated with increased biomarkers of endothelial dysfunction despite viral suppression on long-term antiretroviral therapy in Botswana, Cardiovasc. J. Afr. 29 (2018) 1–7.
[53] K.C. Lund, K.B. Wallace, Direct effects of nucleoside reverse transcriptase inhibitors on rat cardiac mitochondrial bioenergetics, Mitochondrion 4 (2004) 193–202.
[54] A.A. Bulhak, C. Jung, C.-G. Östenson, J.O. Lundberg, P.-O. SjÖquist, J. Pernow, PPAR-α activation protects the type 2 diabetic myocardium against ischemia-reperfusion injury: involvement of the PI3-kinase/Akt and NO pathway, Am. J. Physiol. Circ. Physiol. 296 (2009) H719–H727.